Effect of Light Intensity on the Free-Radical Photopolymerization Kinetics of 2-Hydroxyethyl Methacrylate: Experiments and Simulations

T. Luu, Z. Jia, Andrei Kanaev, L. Museur

The Journal of Physical Chemistry B 2020 124 (31), 6857-6866
DOI: 10.1021/acs.jpcb.0c03140

Effect of Light Intensity on the Free Radical Photopolymerization Kinetics of 2-Hydoxyethyl Methacrylate (HEMA): Experiments and Simulations

T.T.H. Luu [a], Z. Jia [a,b], A. Kanaev [b], L. Museur [a]*

a) Laboratoire de Physique des Lasers CNRS UMR 7538, Université Sorbonne Paris Nord, F-93430, Villetaneuse, France.

b) Laboratoire des Sciences des Procédés et des Matériaux CNRS UPR 3407, Université Sorbonne Paris Nord, F-93430, Villetaneuse, France.

Corresponding Author

* luc.museur@univ-paris13.fr

00 33 1 49 40 37 24

ABSTRACT

The effect of UV light intensity on the kinetics of free radical polymerization 2-hydoxyethyl methacrylate (HEMA) triggered with phenylbis(2,4,6-trimethylbenzoyl)phosphine oxide (BAPO) photoinitiator was investigated experimentally and theoretically. The temporal evolution of the conversion yield and polymerization rate was followed by Raman spectroscopy. The experimental data were treated with a kinetic model, which takes into account significant diffusion controlled processes and termination pathways including bimolecular reaction and primary radical termination. This model showed a very good agreement with the experiment in a large range of the UV light intensities and shed light on the termination process. In particular, it was show that the primary radical termination is dominant for relatively low light intensities below 1 mW/cm², when the photoinitiator is weakly consumed during the polymerization process.

1. INTRODUCTION

Nowadays, polymers became key materials in the development of advanced technologies[1-4]. The free radical polymerization (FRP) is one of the main processes currently used for the production of polymers or polymers based composites. This reaction is triggered by the production of primary radicals as a result of the thermal or photoexcitation of initiating molecules [5]. Compared to thermally induced polymerization, photopolymerization leads to shorter curing times and allows the spatial control of the reaction. 2D and 3D structures with submicrometer resolution can be thus fabricated [6]. The FRP mechanism is the result of a complex interplay between initiation, propagation and termination reactions. All these reactions occur simultaneously. Their rate constants vary significantly as the reaction goes from zero to the complete conversion, resulting in a gradual increase in the viscosity of the reaction mixture by several orders of magnitude. The termination reactions stop the growing of macroradicals, or living radicals, formed during the propagation step. This occurs either by bimolecular reactions as combination, disproportionation or primary radical termination (PRT) either by unimolecular reaction such as radical trapping [5]. The relative proportion of these different mechanisms depends on the functionality of the monomers and is supposed to vary during the formation of the polymer network. Mathematical modeling of the polymerization kinetics and subsequent comparison with experimental measurements enable a better understanding of the interplay between these processes. It gives also access to information difficult to obtain through experiments, such as the evolution of the concentrations of radical species during the FRP reaction. Numerous models have been developed to quantify the effect of diffusion-controlled phenomena on the kinetics of polymerization reactions [7-16]. All these models attribute the autoacceleration of the polymerization rate to the progressive hindering of macroradicals movements by diffusional limitations, resulting in a drastic decrease in the termination rate. Similarly, the autodeceleration observed at higher conversion yield when the reactive medium approaches glass transition, is assigned to the diffusional control of the propagation reaction.

However, most of these models do not take into account the competition between different termination processes, considering only bimolecular processes between macroradicals. Studies analyzing details of the termination modes during FRP process are rare [17-18]. From experimental point of view, common ways for monitoring the FRP kinetics are based on differential scanning calorimetry (DSC) or dilatometry, which are indirect approaches and offer response times of typically 1 second. Conversely, the spectroscopic techniques, such as real-time IR or Raman spectroscopies, allow to monitor the polymerization process by observation of the C=C double bonds opening during the monomer conversion. Their time resolution can be as low as 10 ms allowing polymerization reactions occurring in a fraction of a second to be studied [19]. Moreover, the confocal Raman spectroscopy can also provide a spatial resolution allowing to probe only a few cubic micrometers of the reaction medium [20].

The poly 2-hydoxyethyl methacrylate (pHEMA) is a biocompatible material with many applications in biomedicine for fabrication of artificial coronae, contact lenses, drug delivery systems or tissue engineering [3, 21-23]. Combined with an inorganic component, it is also used to synthesize photoactive hybrids with applications in optoelectronics or sensors technology [24-28]. The FRP of the monomer 2-hydoxyethyl methacrylate (HEMA) with different types of crosslinkers and photoinitiators has been therefore studied for a long time and remains today a topical issue [29-31]. Recently, the ultrafast polymerization of HEMA initiated by high pressure in absence of any initiator molecules, in order to obtain material of ultra-high purity, has been demonstrated[32-33]. Despite its many fields of applications, there are very few studies devoted to the analysis and modelling of HEMA FRP kinetics at high conversion yield. In fact, only Bowman's group has proposed a kinetic model, based on the free volume theory, to describe the polymerization kinetics of HEMA [11-13]. In this model, diffusion controlled phenomena are considered in the expressions of termination and propagation rate constants. A method is also proposed for experimental measurements of key kinetic parameters [34]. This approach has recently been successfully used by Achilias et al [35] to study the thermally activated polymerization of HEMA at different temperatures ($T \geq T_g$) by means of DSC.

However, the validity of this model has never been tested for a large range of initiation rates. The influence of different termination processes and their evolution when FRP kinetics becomes controlled by diffusion phenomena has never been considered either.

In this article we present the experimental analysis and mathematical modeling of bulk free radical photopolymerization kinetics of HEMA. The aim of this study was analyzing both (i) influence of UV light intensity on FRP kinetics and (ii) competition between the different termination pathways. The FRP process was monitored via Raman spectroscopy *in situ*, during UV light irradiation of the reactive medium. The rate of initiation was varied over more than two orders of magnitude by changing the UV intensity. To study how different termination pathways change with the UV light intensity, a detailed kinetic model is proposed, including diffusion controlled initiation, propagation, and termination reaction. It also considers spatiotemporal variations of the photoinitiator and monomer concentrations. All kinetics parameters used in the model were either estimated experimentally or taken from accurate independent measurements found in literature. Thanks to these simulations we quantitatively evaluated concentrations of species in the reaction medium and analyzed how incident light intensity affects termination reactions.

1. METHODS

1.1. Materials

Liquid HEMA with purity >99%, was purchased from Aldrich. Before use, oxygen was removed by repeated freeze /thaw cycles. Liquid HEMA is frozen using liquid nitrogen, then pump under vaccum for few minutes while it is frozen. No further purification has been carried out. Phenylbis(2,4,6-trimethylbenzoyl)phosphine oxide (BAPO, 97%) purchased from Sigma-Aldrich was used as photoinitiator without further purification. It was mixed with HEMA at concentration 0.5 wt% under controlled atmosphere.

1.2. Experimental methods.

The photopolymerization kinetics was studied by means of Raman spectroscopy. The monomers solution is placed, under controlled atmosphere, between two glass plates separated by L = 250 μm using a 1x1 cm adhesive gene frame (Thermo Scientific). This procedure allows avoiding the continuous diffusion of atmospheric oxygen trough the sample during the experiment. The UV light source was a high repetition rate (10 kHz) UV laser delivering pulses of 7 ns at 355 nm and a maximum mean power of 10 mW (CNI MPL-F-355). The laser beam was expended to irradiate the whole surface of the sample (figure S1.a). The UV mean power was adjusted by a set polarizers and measured by thermopile laser power sensor (Coherent PS 10).

All Raman spectra were measured at room temperature in backscattering configuration using a HR800 spectrometer equipped with a Peltier-cooled CCD detector (Horiba JobinYvon) with spectral and spatial resolutions of 0.25 cm^{-1} and 5 μm, respectively. Raman measurements were carried out in-situ by focussing the probe beam at 640 nm in the middle of the sample (see figure S1.a in Electronic Supplementary Information ESI).

The FRP of HEMA was monitored from the progressive decrease of intensity of the C=C bond stretching band at 1640 cm^{-1} of the monomer, simultaneously accompanied by the increase in the C-CH_2 band (1455 cm^{-1}) intensity. The spectra were normalized to the intensity of the C=O band at 1730 cm^{-1}, which was not involved in the polymerization process (figure S1.b in ESI). After the fitting of each Raman spectra with a multi peak function, the conversion yield (CY) of monomer was calculated as [36]:

$$CY = 1 - \frac{\left(I_{C=C} / I_{C=O}\right)_t}{\left(I_{C=C} / I_{C=O}\right)_{t=0}} \quad (1)$$

where $I_{C=C}$ and $I_{C=O}$ are, respectively, the areas of the ν(C=C) and ν(C=O) Raman bands before irradiation and at irradiation time t. To calculate the rate of polymerization the CY is first smoothed

using rlowess algorithm[37]. The normalized rate of polymerization is then obtained directly from the smoothed conversion yield by the expression:

$$R_p = \frac{d\,CY}{dt} \tag{2}$$

In order to have a real time monitoring of the FRP reaction, the Raman spectra were registered each 0.5 s. The spectra were treated in automatic mode by Matlab software and the extracted bands intensities were used to calculate CY. Each experimental series was repeated at least two times to ensure reproducibility of the observed kinetics.

1.3. Computational methods

The set of differential equations describing the modeling of the polymerization reaction has been implemented in MATLAB and numerically solved using ode23s solver. The CY was directly calculated from the concentration of monomer at time *t* and the rate of propagation from equation (2)

2. MODELLING

2.1. Kinetics and mechanisms

Numerous models have been developed to model the kinetics of polymerization reactions [7]. Basically the polymerization of a monomer M initiated by the excitation of a Norrish type-I photoiniator PI can be divided in three main steps

Initiation: $$PI \xrightarrow{h\nu} R_A^{\bullet} + R_B^{\bullet} \tag{3}$$

$$R_A^{\bullet} + M \xrightarrow{k_i^A} P_1^{\bullet} \tag{4}$$

$$R_B^{\bullet} + M \xrightarrow{k_i^B} P_1^{\bullet} \tag{5}$$

Propagation : $$P_n^{\bullet} + M \xrightarrow{k_p} P_{n+1}^{\bullet} \quad (6)$$

Bimolecular termination by combination or disproportionation:

$$P_n^{\bullet} + P_m^{\bullet} \xrightarrow{k_{t,b}} D_{n+m} \text{ or } D_n + D_m \quad (7)$$

where $R_A^{\bullet}$ and $R_B^{\bullet}$ are the primary radicals formed by the photodissociation of PI, $P_n^{\bullet}$ represents the macroradicals containing n monomer units also called "living" polymers, and D_n denotes the "dead" polymer chain also containing n monomers units. The processes described above form the basic model of photoinduced free radical polymerization. To account for the experimental results presented later, additional termination pathway involving primary radical has been also considered. Actually, the primary radicals can also react with the macroradicals by the so called primary radical termination process:

$$R_A^{\bullet} \text{ or } R_B^{\bullet} + P_n^{\bullet} \xrightarrow{k_{t,PRT}} R_A P_n \text{ or } R_B P_n \quad (8)$$

or react with their equivalent to form unreactive dimers, or also recombine to yield PI again:

$$R^{\bullet} + R^{\bullet} \rightarrow R.R \text{ with } R = R_A \text{ or } R_B \quad (9)$$

$$R_A^{\bullet} + R_B^{\bullet} \rightarrow PI \quad (10)$$

2.2. Diffusion –controlled reactions

Termination and propagation. Bowman *et al*. [12-13, 34] have proposed a model to account for the progressive diffusion control of the termination and propagation processes during the polymerization reaction. Actually, diffusion control means that k_p and $k_{t,b}$ are sensitive to the different factors that can affect the viscosity of the reaction medium, such as conversion yield. Actually, the bimolecular termination process is diffusion controlled from the very beginning of the reaction [38]. This reaction is considered to occur in three steps (1) contact between two living radicals as a result of translational diffusion (2) segmental reorientation to bring reactive chains ends in close

proximity and (3) termination reaction itself. At low conversion, the termination rate is controlled by segmental diffusion[39]. The present model has the advantage of being simple and allowing the experimental determination of the different parameters introduced. It is based on the fractional free volume ν_f which represents the fraction of unoccupied volume in the reaction medium. This volume decreases as the reaction proceeds according to:

$$\nu_f = 0.025 + \alpha_M \left(T - T_{g,M}\right)\Phi_M + \alpha_P \left(T - T_{g,P}\right)\left(1 - \Phi_M\right) \tag{11}$$

$$\text{with} \quad \Phi_M = \frac{1 - CY}{1 - CY + CY\left(\rho_M / \rho_P\right)} \tag{12}$$

In the above expressions P and M stands for polymer and monomer respectively, α denotes the coefficient expansion, T_g the glass transition temperature, ρ the density and Φ_M is the volume fraction of monomers. The corresponding values for HEMA are given in table S1 in ESI. The expressions of the propagation (k_p) and bimolecular termination ($k_{t,b}$) rate constants are then given by :

$$\frac{1}{k_p} = \frac{1}{k_{p0}} + \frac{1}{k_{p0}\ \exp\left(-A_p\left(\frac{1}{\nu_f} - \frac{1}{\nu_{f,cp}}\right)\right)} \tag{13}$$

$$\frac{1}{k_{t,b}} = \frac{1}{k_{t,b0}} + \frac{1}{k_{t,res} + k_{t,b0}\exp\left(-A_t\left(\frac{1}{\nu_f} - \frac{1}{\nu_{f,ct}}\right)\right)} \tag{14}$$

In these expressions, k_{p0} and $k_{t,b0}$ stands for initial rates constants, i.e. at the very beginning of the reaction. The exponential factors A_p and A_t govern the rate at which propagation and termination rate constants decrease with viscosity. Finally, the bimolecular propagation and termination processes become diffusion-limited when the fractional free volume reaches the values $\nu_{f,cp}$ and $\nu_{f,ct}$ respectively. In equation (14) $k_{t,res}$ describes the contribution of the reaction-diffusion process

on the termination rate constant. Indeed, when macroradical chains are immobilized due to the increase of viscosity, the radical sites can continue to propagate through unreacted double bonds until they encounter another macroradical. A normal bimolecular termination reaction (eq.(7)) then occurs between the two radicals. The corresponding rate constant $k_{t,res}$ is proportional to the propagation rate constant and double bond concentration:

$$k_{t,res} = R_{rd} k_p [M] \quad (15)$$

where R_{rd} is the reaction-diffusion parameter. In equation (14), the rate constant $k_{t,b}$ is considered for bimolecular terminations since the mode of termination, by combination or disproportionation, does not influence the kinetics. Moreover, the polydispersity of macroradical chains length should lead to a large spread of termination rates. The termination rate constant $k_{t,b}$ considered in this modelling is therefore an average over all macroradicals chain-length. All these parameters can be determined experimentally from the measurement of the polymerization rate [34].

Initiation. The polymer network growth affects the initiation reactions (eq. (4) and (5)), which underwent diffusional limitation. Since these processes involve the diffusion of a small radical molecules, their rate constants k_i^A and k_i^B are considered to have the same form as k_p (eq.(13)) [11-12]. Thus, we assume that $A_i = A_p$ and $\nu_{f,ci} = \nu_{f,cp}$. The values of the intrinsic initiation rate constants k_{i0}^A and k_{i0}^B found in literature are given in table S1 in ESI.

Primary radical termination. The primary radical termination mechanism also involves the diffusion of small molecules. Using the same argument as above, the rate constant $k_{t\,PRT}$ can be considered to have the same form than k_p (eq.(13)) [11-12]. Therefore, we assume that $A_{TPR} = A_p$ and $\nu_{f,c\,TPR} = \nu_{f,cp}$. Moreover, the primary free-radical termination process is supposed to be diffusion controlled from the very beginning of the reaction. Its initial rate constant ($k_{t,PRT\,0}$) is therefore set equal to the diffusion constant ($k_{diff\,0}$) given by :

$$k_{t,PRT\,0} = k_{diff\,0} = \frac{8RT}{\eta_0} \tag{16}$$

where T is the temperature, R is gas constant and η_0 is the macroscopic viscosity of the initial monomer solution.

The detailed material balances equations corresponding to processes described by eq.(3)-(8) are given in ESI (table S2).

3. RESULTS.

3.1. Experiments

Photopolymerization experiments have been carried out for UV light intensities covering a broad range from 0.01 mW/cm^2 to 3 mW/cm^2. Under this irradiation, BAPO dissociates to form phosphinoyl ($R_A^\bullet$) and benzoyl ($R_B^\bullet$) radicals, which react with monomers initiating the polymerization reaction (eqs (4)-(5)). The initiation by each of these radicals takes place at different stages of the process because of much different rate constants $k_{i0}^A = 6 - 11\text{x}10^7\ M^{-1}s^{-1}$ and $k_{i0}^B = 0.9\,\text{x}10^5\ M^{-1}s^{-1}$ [40] and phosphinoyl is consumed first. The effect of incident light intensity on the measured conversion yield (*CY)* and rate of polymerization R_p are respectively reported in figures 1 and 2 respectively. Our results showed that the maximum conversion yield CY_{max} = 0.72 ± 0.03 does not depend on the light intensity. On the other hand, as figure 2 shows, relatively low intensities ≤1 mW/cm² accelerate the reaction kinetics, which results in attaining CY_{max} at earlier times. In contrast, at relatively high intensities above 1 mW/cm^2, the rate of polymerization approaches a constant value (shown in inset of figure 2). In the frame of the steady state approximation, and considering only bimolecular macroradicals termination mechanisms, the rate of polymerization R_p scales with the square root of the initiation rate:

$$R_p = k_p[M]\left(\frac{R_i}{2k_t}\right)^{0.5} \quad \text{with } R_i = 2f_0\phi\alpha[PI]I_0 e^{-\alpha[PI]L/2} \tag{17}$$

where R_i is the local rate of initiation at the position $x = L/2$ inside the reaction medium, ϕ the dissociation quantum yield of the photoinitiator, f_0 the initiator efficiency, α the photoinitiator absorption coefficient and I_0 the incident UV light intensity. The experimentally measured rate of polymerization deviates from this ½ power law and saturates when UV light intensity exceeds 0.5mW/cm^2. Since the rate of PRT process is independent of light intensity, the observed limitation of R_p can be assigned to a growing contribution of primary radicals on the termination reactions (eq.(8)) [11, 18].

The reaction autoacceleration, characteristic of the polymerization process, can be also observed in figures 1 and 2. In fact, in the process beginning the polymerization rate is almost constant and then increases much faster. This effect is generally attributed to a progressive restriction of the segmental and translational mobility of the macroradicals in course of the polymerization process, while the mobility of the small monomers is conserved. A consequent decrease of the termination rate leads to an accumulation of macroradicals and, therefore, to an increase of the propagation rate up to a maximum value $R_{p,\ max}$. At higher conversion yield, an increase of viscosity and vitrification of medium restrict the mobility of monomers. In these conditions, the rate constant k_p decreases as well as the rate of polymerization.

Compared to differential scanning calorimetry, the use of spectroscopic approaches to probe the kinetics of polymerization reaction, as NIR absorption or Raman scattering, cannot ensure that isothermal conditions are met because of the absence of temperature control. However, in the present experiments we suppress the temperature variations by using a thin slab sample (of 250 microns thickness) and relatively low UV light power (<3mW/cm2), which sets the reaction half-times (time to reach 50% of conversion) to 40 s or longer. Two experimental observations support the assumption of small temperature variations in the reaction media. (i) The variation of CY with time is the same wherever the sample is analyzed, even close to the interface where convection cooling is most efficient. (ii) The maximum conversion yield CY_{max} does not depend on the UV light power,

indicating that the polymerization reactions occur at similar temperatures. Moreover, simulations and experiments performed by other groups also support the assumption of a low temperature increase in our experimental experiments. For example, Lecamp et al. [41] have simulated the heat transfer during the polymerization reaction in a 200 µm thin film of dimethacrylate monomers with polymerization enthalpy of 115 J/g. They have concluded that the temperature increase in the film does not exceed 1 °C when the reaction half-time is longer than 10 s. By studying polymerization of the same dimethacrylate monomer, Kerbouc'h et al. [42] have reported the temperature increase by 5 °C in a sample of 2 mm thickness irradiated at 365 nm with 1 mW/cm2 power. Although, the polymerization enthalpy of HEMA is higher (420 J/g), the heat release is compensated by a slower release of heat (half-time of reaction ranging from 40s to 300s) and a finer sample, allowing a low temperature increase to be assumed in the present experiments.

3.2. Simulations

In this modeling, the UV pulsed laser used to initiate the reaction is considered as a CW light source. Indeed, the rate of side reactions between primary radicals, which might occur during irradiation with high intensities, is negligible. Given a mean laser power of 10 mW and a repetition rate of f_L = 10kHz, the maximum concentration of radicals generated in one laser pulse can be estimated to $[R^\bullet] = 3.10^{-7}\,\mathrm{M}$. The reactions between primary radicals (eqs. (9) and (10)) are diffusion controlled and their rate can be expressed as $R_{rad-rad} = k_{diff}[R^\bullet]^2$, whereas the rate of initiation is $R_i = k_{i0}[R^\bullet][M]$. Assuming diffusion and initiation rate constants equal to $k_{diff} = 10^9$ and $k_{i0} = 10^5$ $M^{-1}.s^{-1}$ respectively, we conclude that $R_i >> R_{rad-rad}$. In the range of fluencies used in this experiment, a primary radical is therefore more likely to react with a highly concentrated monomer double bond C=C ($[M]_0 = 8.25\,M$) than with any another primary radical. Moreover, considering a propagation rate constant $k_p = 10^3$ $M^{-1}.s^{-1}$ and assuming a living radical concentration

of $[P_n^\bullet] = 10^{-1} M$, one can see that the characteristic time of disappearance of monomers $\tau = \left(k_p [P_n^\bullet]\right)^{-1}$ is much larger than the time between two laser pulses $\tau >> 1/f_L$.

The mathematical model used to describe the photopolymerization reaction requires knowledge of several process parameters. Some of these data, listed in table S1 in ESI, were found in literature and another were obtained directly in present experiments. The rate constants k_{p0} and $k_{t,b0}$ governing the evolution of the polymerization rate in the process beginning can be evaluated at low conversion yields, when the photoinitiator concentration and propagation and termination kinetics rate constants can be assumed to be constant [35]. In these conditions, integration of eq. (17) results in:

$$-\ln(1-CY) = k_{eff}\, t \quad \text{with} \quad k_{eff} = k_{p0}\left(\frac{f_0\, \phi\, \alpha [PI]_0\, I_0\, e^{-\alpha [PI]_0 L/2}}{k_{t,b0}}\right)^{0.5} \tag{18}$$

A linear fit of $\ln(1\text{-}CY)$ as function of time for different intensities I_0, allows to obtain $k_{p0}\sqrt{f_0 \phi / k_{t,b0}}$, as shown in figure 3, since values of all the other parameters in eq. (18) are known (see table S1 in ESI). For intensities ranging from 0.01 to 1 mW/cm^2, this value is constant $k_{p0}\sqrt{f_0 \phi / k_{t,b0}} = 0.72\ (M^{-1} s^{-1})^{1/2}$. Using the rate constant of propagation measured by Buback *et al.* $k_{p0} = 1288 M^{-1} s^{-1}$ [43], $f_0 = 1$ and $\phi = 0.5$ [44-45], the termination rate constant $k_{t,b0} = 1.60.10^6 M^{-1} s^{-1}$ can be estimated. This value is very close to that proposed in Ref. [34]. For UV intensities higher than 1mW/cm^2 this same ratio decreases. Since the intrinsic rate constants k_{p0}, $k_{t,b0}$ and quantum yield of photoinitiator dissociation ϕ are not expected to change, we concluded that the radical efficiency factor f_0 decreases when UV intensity increases. This means that a larger fraction of radicals formed in the primary step of the initiator decomposition participates in side reactions that do not lead to formation of the polymer chains. The values $f_0 = 0.73$ and $f_0 = 0.41$ have been respectively obtained for the light intensities 2 and 3 mW/cm^2. Since primary radical

recombination reaction are unlucky in our experimental conditions, the so-called induced decomposition of initiator could be responsible of the wastage of photoinitiator molecules [5]. In this chain transfer reaction, the attack of initiators by propagating radicals leads to the formation of one radical $P_n^{\bullet} + PI \rightarrow P_n R' + R^{\bullet}$. The rate of this process is proportional to the concentration in living radicals $[P_n^{\bullet}]$ and increases with the rate of initiation. However, due to the lack of data for the photoinitiator and monomer considered in this study, further experiments are required to confirm the exact role of this process. Complementarily to the above rate constants, kinetic parameters R_{rd} A_p, A_t, $\nu_{f,cp}$ and $\nu_{f,ct}$ describing the diffusion controlled propagation and termination reactions were determined and compared in a large range of UV light intensities. This was done following a procedure proposed in [34-35] and described in ESI. The obtained kinetics parameters are shown in figure 4 and summarized in table S3 of ESI. As explained above, these kinetics parameters are also used in the expressions of the initiation and PRT rates constants.

The calculated CY and rate of polymerization R_p based on the above determined kinetic parameters are shown in figures 1 and 2, including (continuous line) and not (dash line) the PRT mechanism. For low UV light intensity 0.1 mW/cm^2, both simulations well predict variations of CY and R_p with time. However, when the intensity increases the difference between the two predictions becomes significant. We notice that neglecting PRT process, the simulation tends to overestimate the conversion yield in the vicinity of glassy transition. In contrast, our modelling including PRT successfully described CY and R_p with a tolerance of few percent in the whole range of UV intensities.

4. DISCUSSION

According to figure 4, the reaction-diffusion constant R_{rd} is the only parameter strongly affected by the UV light intensity: it increases almost a factor of 10 to the end of the process. On the other hand, A_t and $\nu_{f,cp}$ slightly decrease, and A_p and $\nu_{f,ct}$ seem not affected by the change of UV

intensity. The propagation k_p and bimolecular termination $k_{t,b}$ rate constants calculated using parameters of table S3 (ESI) as function of the CY are plotted in Figure 5. In order to validate the results of these simulations, the rate constants k_p and $k_{t,b}$ were also measured experimentally in a series of independent experiments combining steady state and non-steady state analysis [46-47] (see ESI). The values obtained when the UV light intensity is equal to 1 mW/cm^2, are represented by symbols in figure 5. They are in good agreement with the rate constants calculated from the model. The variation of rate constants during the polymerization reaction can be discussed as follow. The propagation rate constant k_p remains constant as long as the mobility of the monomers is not impeded by the formation of the polymer network; it then decreases when the glass effect occurs. One can see that higher is the light intensity higher is the conversion yield value, from which the monomers mobility is reduced. This can be related to the molecular weight of the produced polymers. The kinetics chain length $\nu = M_0 R_p / R_i$, i.e. the number of time a radical participates in a propagation reaction, decreases when the rate of initiation increases. Thus, short and more numerous polymers chains formed at high UV intensities have a smaller effect on the monomers mobility compared to the longer chains formed at low UV intensities. The rate constant of bimolecular termination $k_{t,b}$ in figure 5 shows a more complex behavior. However, the diffusion control of the reaction also in this case occurs at higher conversion rate when the intensity increases. Consequently, large concentrations of short macroradicals chains (generated at high light intensities) facilitate bimolecular termination reactions. From its initial value $k_{t,b0}$ the rate constant of termination drops by two orders of magnitude at $CY \geq 0.25 - 0.3$, when the movement of radicals becomes the rate-determining step leading to an increase of the polymerization rate. The rate constant of termination is then proportional to the rate constant of propagation and monomers concentration (eq. (15)). At higher CY, $k_{t,b}$ further decreases proportionally to k_p when the propagation becomes fully diffusion controlled.

When the UV intensity increases the reaction-diffusion constant R_{rd} increases from 0.5 to 3.7 L/mol (figure 4). This last value is in agreement with the value $R_{rd} = 4$ L/mol reported in [13] for photopolymerization of HEMA carried out under UV (365 nm) light intensity of 4 mW/cm^2. Nevertheless, the evolution of the reaction-diffusion constant R_{rd} with the intensity deserves an additional discussion. Russell *et al.* have proposed two limiting equations for the estimation of R_{rd} [48]. The first equation gives a minimum value $R_{rd,\,min}$ supposing that polymer chain ends are rigid and the second equation predicts a maximum value $R_{rd,\,max}$ when chain ends are supposed totally flexible:

$$R_{rd,\,\min} = \frac{2\pi}{3} a^2 \sigma \frac{N_A}{1000}$$
$$R_{rd,\,\max} = \frac{4\pi}{3} a^3 \, j_c^{1/2} \frac{N_A}{1000} \qquad (19)$$

Here a is the root-mean-square end-to-end distance per square root of the number of monomers units, σ is the Lennard-Jones diameter of the monomer and j_c is the distance between entanglement in monomer units, where j_c is related to the entanglement spacing in pure polymer j_{c0} by the relation $j_c = j_{c0} / (1-\phi_m)$ [49]. These parameters are tabulated in literature and their values are reported in table S1 of ESI. The use of eq. (19) results in $R_{rd,\,\min} = 0.36$ and $R_{rd,\,\max} = 9.15$ in case of HEMA. The values of R_{rd} found in the present work lie between these two limits. . The observed increase of R_{rd} with the light intensity may indicate a transition from rigid to flexible chain ends. The reaction-diffusion constant can be consequently considered as a measure of the radical mobility, related to the kinetics chain length varied from 80000 at 0.01 mW/cm^2 to 4000 at 3 mW/cm^2. We notice that polymerization experiments performed with thermally activated initiator may support this interpretation. Indeed, the decrease of the reaction diffusion constant and, therefore, transition to a more rigid system were observed when the reaction temperature increases [35, 50]. This *a priori* counterintuitive effect, correlates well with the reduction of the kinetic chain length when the temperature, and the rate of initiation, increase.

The modelling allowed understanding the evolution of reactive species in the polymerized medium, which generally escape in situ observations. In the following we discuss changes in the termination mechanism when the rate of initiation increases. Resuming our previous considerations, two different termination reactions can occur during FRP: (1) bimolecular reactions between two macroradicals, either by combination or disproportionation mechanisms, leading to the formation of dead polymers chains D_n (eq.(7)), and (2) reactions between a macroradical, $P_n^\bullet$ and a primary radical, $R_A^\bullet$ or $R_B^\bullet$, leading to dead polymer chains denoted $R_{A\,or\,B}P_n$ (eq.(8)). At the end of the process, remaining nonreacted macroradicals $P_n^\bullet$ are trapped by occlusion in the polymer network underwent vitrification [17]. The evolution, of fractions of macroradicals $P_n^\bullet$, terminated species D_n and R_BP_n, as well as the relative BAPO concentration [BAPO]/[BAPO]$_0$ are represented in figure 6 as a function of conversion yield, traced until the maximum experimental value of CY_{max} =0.72. Because of much higher initiation reaction constant ($k_{i0}^A >> k_{i0}^B$), phosphinoyl radicals $R_A^\bullet$ radicals are mainly consumed in initiation reactions and mainly benzoyl radicals $R_B^\bullet$ participate late in PRT reactions. This assumption was confirmed by modelling showed that the concentration of $[R_BP_n]$ is three orders of magnitude higher than that of $[R_AP_n]$ (figure S3 of ESI). Therefore, the very low proportion of R_AP_n species is not represented in figure 6. As one can see, when $CY < 0.55$ the polymerization reaction essentially produces polymer chains D_n terminated by bimolecular reactions. The PRT process is not effective in this range of low conversion yields. A small decrease of the amount of D_n chains in this range is explained by a progressive diminution of the propagation rate constant k_p and, therefore, termination rate constant $k_{t,b}$ (see Figure 5). Since no other termination process is efficient, the decrease of D_n concentration is correlated with the increase of macroradicals $P_n^\bullet$ concentration. This decrease of [D_n] weakened at higher UV light intensities, when the diffusional limitation of k_p occurred at higher values of *CY* (figure 5). The PRT process becomes efficient only on the last stage of the polymerization process. Indeed, independently on the light intensity the fraction

of $R_B P_n$ chains increases continuously from *CY = 0.55*. Table 1 reports fractions of terminated species and macroradicals at the end of polymerization process when *CY* attains CY_{max} =0.72. Surprising, the final fraction of macroradical continuously decreases as the UV intensity increases. Indeed, because of a faster medium vitrification, an higher light intensity is supposed to promote radical trapping [51]. One would also expect $R_B P_n$ chain fraction to increase at UV high light intensities, due to a higher concentration of primary radicals. Instead, it increased between 0.01 and 0.1 mW/cm^2, remained stable up to 1 mw/cm^2 and decreased when I_{uv} = 3 mw/cm^2. There is also no marked trends in the evolution of the polymer chains fraction D_n: it varied very little when I_{uv} increased from 0.01 to 1 mW/cm^2 (28-35%), and increased up to 69% when I_{uv} = 3 mW/cm^2. As explained below, fractions of terminated species critically depend on the photoinitiator concentration at the end of the process.

Since the initial value of the rate constant of the primary radical termination process is higher than that of bimolecular termination process $k_{t,PRT0} >> k_{t,b0}$, it may seem surprising that the primary radical termination becomes the main termination pathway only at high conversion yield. Actually at the beginning of the reaction primary radicals $R_A^\bullet$ and $R_B^\bullet$ are mainly involved in initiation reactions, because the concentration of monomers is high compared to those of radicals: $k_i[M][R^\bullet] >> k_{t,\,PRT}[P_n^\bullet][R^\bullet]$. Only when the bimolecular termination process becomes strongly limited by diffusion, leading to an increase of the living radicals concentration $[P_n^\bullet]$, the primary radicals termination process can become significant. More precisely, the effectiveness of PRT process depends on two factors: (i) consumption of photoinitiator molecules and (ii) competition between PRT and initiation reactions. This last factor can be expressed by a ratio between PRT and initiation rates [17]:

$$\frac{R_{PRT}}{R_i} = \frac{k_{t,\,PRT}[P_n^\bullet][R^\bullet]}{k_i[M][R^\bullet]} = \frac{k_{t,PRT0}[P_n^\bullet]}{k_{i0}[M]} \qquad (20)$$

where $R^{\bullet} = R_A^{\bullet}$ or $R_B^{\bullet}$. In frame of the proposed model, initiation and PRT kinetics are controlled by the rate constants k_i and $k_{t,PRT}$ functionally varying in the same way during polymerization process. In these conditions, the ratio R_{PRT} / R_i is nearly proportional to the concentration of macroradicals $[P_n^{\bullet}]$. Figure 7 depicts variation of R_{PRT} / R_i for benzoyl radical $R_B^{\bullet}$ as a function of conversion yield. For a given conversion yield, the ratio R_{PRT} / R_i increases when UV light intensity increases from 0.01 to 1 mW/cm^2. However, when I_{UV} = 3 mW/cm^2 this ratio begins to decrease. This affects the production of $R_B^{\bullet}$ radicals, and consequently of macroradicals, which falls at high conversion yields when UV light intensity increases (see figure S4.b in ESI). Consequently, the benzoyl primary radical concentration decreases as it is shown on the insert of figure 7. Accordingly, ratio R_{PRT} / R_i decreases as well. The PRT reactions stopped when the photoinitiator is fully consumed. The remaining macroradicals then slowly recombine through still active bimolecular terminations. As a result, their fraction decreases while that of polymer chains D_n increases. Our calculations also confirmed that ratio R_{PRT} / R_i for phosphinoyl radicals $R_A^{\bullet}$ is extremely low (figure 7) and these radicals are not involved in the PRT process.

Christmann *et al.* [17] have recently calculated photopolymerization kinetics of diacrylate monomer initiated by type-1 photoinitiator. They have underlined an importance of the diffusion control reactions and photoinitiator consumption on radical termination processes pathways, which confirm results of the present study. On the other hand, they have concluded that bimolecular termination is always remained the major termination reaction. Our results show that the situation can be more complex in case of a photoinitiator, which decomposition leads to the formation of two radicals with strongly different initiation activities. In these conditions, the more active radical mainly participates in the initiation reactions, while the radical with a smaller activity is involved in the termination reactions taking place at the late stage of the polymerization process. This effect should be taken into account by choice of a photoinitiator molecule.

We notice that many side reactions could complete modeling of the polymerization process, as e.g. macroradicals trapping, chain transfer to monomer, etc. This however may introduce a number of unknown parameters, which cannot be directly measured. Our model used a significant set of processes sufficient for the description of FRP kinetics. Another point to notice is the beneficial using high UV light intensities. We showed that while final conversion yield does not depend on the intensity, the polymer composition strongly depend on it. In practice, the use of high UV light intensities allows to reduce the fraction of trapped radicals in the polymer sample, which can be of interest for biomedical applications.

5. CONCLUSION.

In this work, kinetics of free radical photopolymerization of HEMA was studied experimentally and theoretically modelled in a broad range of UV light intensities from 0.01 to 3 mW/cm^2. The in situ measurements of the monomer conversion yield were performed by Raman spectroscopy. The kinetic model was taken into account major diffusion controlled reactions (initiation and termination) and termination pathways (bimolecular and via primary radical); all process parameters used in the modelling were found in literature and experimentally measured in this work. A very good agreement between the experiment and modelling was obtained. The results confirm an enhancement of the diffusion control chains propagation and termination processes with an increase of the light intensity, which was assigned to a decrease of the kinetic chain length. The diffusion controlled propagation and termination reactions and consumption of photoinitiator are two main mechanisms affecting the process kinetics. Moreover, the primary radical termination becomes the principal termination process if photoinitiator is not completely consumed during the reaction. Our results show that phosphinoyl and benzoyl radicals released following BAPO photoinitiator decomposition affect respectively mainly initiation and termination reactions because of their much different chemical activities. We showed that composition of final polymer strongly

depend on the light intensity, effectively reducing amount of trapped radicals in the polymer sample at high UV light intensities.

SUPPORTING INFORMATIONS

Scheme of experimental arrangement, values of physical parameters used in the modelling, materials balance equations, rate of polymerization vs conversion yield at different UV intensities, method of determination of kinetics parameters, values of kinetic parameters, evolution of the concentrations of terminated species and macroradicals vs time at different UV intensity, concentration of macroradicals and photoinitiator as function of conversion yield.

ACKNOWLEDGEMENT

ANR (Agence Nationale de la Recherche) and CGI (Commissariat à l'Investissement d'Avenir) are gratefully acknowledged for their financial support of this work through Labex SEAM (Science and Engineering for Advanced Materials and devices), ANR-10-LABX-0096 and ANR-18-IDEX-0001.

ADDITIONAL INFORMATION

Competing Financial Interest: The authors declare no competing financial interests.

REFERENCES

1. Carpi, F.; De Rossi, D.; Kornbluh, R.; Pelrine, R. E.; Sommer-Larsen, P., *Dielectric Elastomers as Electromechanical Transducers: Fundamentals, Materials, Devices, Models and Applications of an Emerging Electroactive Polymer Technology*. Elsevier: **2011**.

2. Belgacem, M. N.; Gandini, A., *Monomers, Polymers and Composites from Renewable Resources*. Elsevier: **2011**.

3. He, W.; Benson, R., Polymeric Biomaterials. In *Applied Plastics Engineering Handbook*, Elsevier: **2017**; pp 145-164.

4. Aguilar, M. R.; San Román, J., *Smart Polymers and Their Applications*. Woodhead Publishing: **2019**.

5. Odian, G., *Principles of Polymerization*. John Wiley & Sons: **2004**.

6. Farsari, M.; Chichkov, B. N., Materials Processing: Two-Photon Fabrication. *Nat Photon* **2009,** *3*, 450.

7. Achilias, D. S., A Review of Modeling of Diffusion Controlled Polymerization Reactions. *Macromolecular Theory and Simulations* **2007,** *16*, 319-347.

8. Terrones, G.; Pearlstein, A. J., Effects of Kinetics and Optical Attenuation on the Completeness, Uniformity, and Dynamics of Monomer Conversion in Free-Radical Photopolymerizations. *Macromolecules* **2001,** *34*, 8894-8906.

9. Terrones, G.; Pearlstein, A. J., Effects of Optical Attenuation and Consumption of a Photobleaching Initiator on Local Initiation Rates in Photopolymerizations. *Macromolecules* **2001,** *34*, 3195-3204.

10. Goodner, M. D.; Bowman, C. N., Development of a Comprehensive Free Radical Photopolymerization Model Incorporating Heat and Mass Transfer Effects in Thick Films. *Chemical Engineering Science* **2002,** *57*, 887-900.

11. Goodner, M. D.; Bowman, C. N., Modeling Primary Radical Termination and Its Effects on Autoacceleration in Photopolymerization Kinetics. *Macromolecules* **1999,** *32*, 6552-6559.

12. Goodner, M. D.; Bowman, C. N. In *Modeling and Experimental Investigation of Light Intensity and Initiator Effects on Solvent-Free Photopolymerizations*, ACS Symposium Series, AMERICAN CHEMICAL SOCIETY: 1998; pp 220-231.

13. Kannurpatti, A. R.; Goodner, M. D.; Lee, H. R.; Bowman, C. N. In *Reaction Behavior and Kinetic Modeling Studies of" Living" Radical Photopolymerizations*, ACS Symposium Series, AMERICAN CHEMICAL SOCIETY: 1997; pp 51-62.

14. Buback, M., Free-Radical Polymerization up to High Conversion. A General Kinetic Treatment. *Die Makromolekulare Chemie: Macromolecular Chemistry and Physics* **1990,** *191*, 1575-1587.

15. Buback, M.; Huckestein, B.; Russell, G. T., Modeling of Termination in Intermediate and High Conversion Free Radical Polymerizations. *Macromolecular Chemistry and Physics* **1994,** *195*, 539-554.

16. Louie, B. M.; Carratt, G. M.; Soong, D. S., Modeling the Free Radical Solution and Bulk Polymerization of Methyl Methacrylate. *Journal of Applied Polymer Science* **1985,** *30*, 3985-4012.

17. Christmann, J.; Ley, C.; Allonas, X.; Ibrahim, A.; Croutxé-Barghorn, C., Experimental and Theoretical Investigations of Free Radical Photopolymerization: Inhibition and Termination Reactions. *Polymer* **2019,** *160*, 254-264.

18. Ibrahim, A.; Maurin, V.; Ley, C.; Allonas, X.; Croutxe-Barghorn, C.; Jasinski, F., Investigation of Termination Reactions in Free Radical Photopolymerization of Uv Powder Formulations. *European Polymer Journal* **2012,** *48*, 1475-1484.

19. Decker, C.; Masson, F.; Bianchi, C., Kinetic Study of Photoinitiated Polymerization Reactions by Real-Time Infrared Spectroscopy. In *In Situ Spectroscopy of Monomer and Polymer Synthesis*, Springer: **2003**; pp 109-124.

20. Yadav, A. K.; Krell, M.; Hergeth, W.-D.; de la Cal, J. C.; Barandiaran, M. J., Monitoring Polymerization Kinetics in Microreactors by Confocal Raman Microscopy. *Macromolecular Reaction Engineering* **2014,** *8*, 543-549.

21. Chirila, T. V., An Overview of the Development of Artificial Corneas with Porous Skirts and the Use of Phema for Such an Application. *Biomaterials* **2001,** *22*, 3311-3317.

22. Anderson, D. G.; Levenberg, S.; Langer, R., Nanoliter-Scale Synthesis of Arrayed Biomaterials and Application to Human Embryonic Stem Cells. *Nature Biotechnology* **2004,** *22*, 863-866.

23. Montheard, J.-P.; Chatzopoulos, M.; Chappard, D., 2-Hydroxyethyl Methacrylate (Hema): Chemical Properties and Applications in Biomedical Fields. *Journal of Macromolecular Science, Part C: Polymer Reviews* **1992,** *32*, 1-34.

24. Garcia, O.; Garrido, L.; Sastre, R.; Costela, A.; García-Moreno, I., Synthetic Strategies for Hybrid Materials to Improve Properties for Optoelectronic Applications. *Advanced Functional Materials* **2008,** *18*, 2017-2025.

25. Yetisen, A. K.; Butt, H.; Yun, S.-H., Photonic Crystal Flakes. *Acs Sensors* **2016,** *1*, 493-497.

26. Evlyukhin, E.; Museur, L.; Diaz-Gomez-Trevino, A.; Traore, M.; Brinza, O.; Zerr, A.; Kanaev, A., Synthesis of Organic–Inorganic Hybrids Via a High-Pressure-Ramp Process: The Effect of Inorganic Nanoparticle Loading on Structural and Photochromic Properties. *Nanoscale* **2018,** *10*, 22293-22301.

27. Uklein, A.; Gorbovyi, P.; Traore, M.; Museur, L.; Kanaev, A., Photo-Induced Refraction of Nanoparticulate Organic-Inorganic Tio2-Phema Hybrids. *Optical Materials Express* **2013,** *3*, 533-545.

28. Gorbovyi, P.; Uklein, A.; Tieng, S.; Brinza, O.; Traore, M.; Chhor, K.; Museur, L.; Kanaev, A., Novel Nanostructured Phema-Tio2 Hybrid Materials with Efficient Light-Induced Charge Separation. *Nanoscale* **2011,** *3*, 1807-1812.

29. Ning, L.; Xu, N.; Xiao, C.; Wang, R.; Liu, Y., Analysis for the Reaction of Hydroxyethyl Methacrylate/Benzoyl Peroxide/Polymethacrylate through Dsc and Viscosity Changing and Their Resultants as Oil Absorbent. *Journal of Macromolecular Science, Part A* **2015,** *52*, 1017-1027.

30. Passos, M. F.; Dias, D. R. C.; Bastos, G. N. T.; Jardini, A. L.; Benatti, A. C. B.; Dias, C. G. B. T.; Maciel Filho, R., Phema Hydrogels. *Journal of Thermal Analysis and Calorimetry* **2016,** *125*, 361-368.

31. Boazak, E. M.; Greene, V. K., Jr.; Auguste, D. T., The Effect of Heterobifunctional Crosslinkers on Hema Hydrogel Modulus and Toughness. *PLOS ONE* **2019,** *14*, e0215895.

32. Evlyukhin, E.; Museur, L.; Traore, M.; Perruchot, C.; Zerr, A.; Kanaev, A., A New Route for High-Purity Organic Materials: High-Pressure-Ramp-Induced Ultrafast Polymerization of 2-(Hydroxyethyl)Methacrylate. *Scientific Reports* **2016,** *5*, 18244.

33. Evlyukhin, E.; Museur, L.; Traore, M.; Nikitin, S.; Zerr, A.; Kanaev, A. V., Laser Assisted High Pressure Induced Polymerization of 2-(Hydroxyethyl) Methacrylate. *The Journal of Physical Chemistry B* **2015,** *119*, 3577-3582.

34. Goodner, M. D.; Lee, H. R.; Bowman, C. N., Method for Determining the Kinetic Parameters in Diffusion-Controlled Free-Radical Homopolymerizations. *Industrial & Engineering Chemistry Research* **1997,** *36*, 1247-1252.

35. Achilias, D.; Siafaka, P., Polymerization Kinetics of Poly (2-Hydroxyethyl Methacrylate) Hydrogels and Nanocomposite Materials. *Processes* **2017,** *5*, 21.

36. Evlyukhin, E.; Museur, L.; Traore, M.; Nikitin, S. M.; Zerr, A.; Kanaev, A., Laser-Assisted High-Pressure-Induced Polymerization of 2-(Hydroxyethyl)Methacrylate. *The Journal of Physical Chemistry B* **2015,** *119*, 3577-3582.

37. Matlab Https://Fr.Mathworks.Com/Help/Curvefit/Smoothing-Data.Html. (accessed may 2020).

38. Sedao, X.; Maurice, C.; Garrelie, F.; Colombier, J.-P.; Reynaud, S.; Quey, R.; Pigeon, F., Influence of Crystal Orientation on the Formation of Femtosecond Laser-Induced Periodic Surface Structures and Lattice Defects Accumulation. *Applied Physics Letters* **2014,** *104*, 171605.

39. Sedao, X.; Maurice, C.; Garrelie, F.; Colombier, J.-P.; Reynaud, S.; Quey, R.; Blanc, G.; Pigeon, F., Electron Backscatter Diffraction Characterization of Laser-Induced Periodic Surface Structures on Nickel Surface. *Applied Surface Science* **2014,** *302*, 114-117.

40. Allen, N. S., *Photochemistry and Photophysics of Polymeric Materials*. John Wiley & Sons: **2010**.

41. Lecamp, L.; Lebaudy, P.; Youssef, B.; Bunel, C., Simulation of Temperature Distributions within Monomer Film During Photopolymerization. *Journal of Thermal Analysis and Calorimetry* **1998,** *51*, 889-896.

42. Kerbouc'h, P.; Lebaudy, P.; Lecamp, L.; Bunel, C., Numerical Simulation to Correlate Photopolymerization Kinetics Monitoring by Rt-Nir Spectroscopy and Photocalorimetry. *Thermochimica Acta* **2004,** *410*, 73-78.

43. Buback, M.; Kurz, C. H., Free-Radical Propagation Rate Coefficients for Cyclohexyl Methacrylate, Glycidyl Methacrylate and 2-Hydroxyethyl Methacrylate Homopolymerizations. *Macromolecular Chemistry and Physics* **1998,** *199*, 2301-2310.

44. Jockusch, S.; Koptyug, I. V.; McGarry, P. F.; Sluggett, G. W.; Turro, N. J.; Watkins, D. M., A Steady-State and Picosecond Pump-Probe Investigation of the Photophysics of an Acyl and a Bis (Acyl) Phosphine Oxide. *Journal of the American Chemical Society* **1997,** *119*, 11495-11501.

45. Eibel, A.; Fast, D. E.; Gescheidt, G., Choosing the Ideal Photoinitiator for Free Radical Photopolymerizations: Predictions Based on Simulations Using Established Data. *Polymer Chemistry* **2018,** *9*, 5107-5115.

46. Decker, C.; Moussa, K., Photopolymerisation De Monomeres Multifonctionnels—Iii. Analyse Cinetique Par Spectroscopie Infrarouge Resolue Dans Le Temps (Rtir). *European Polymer Journal* **1990,** *26*, 393-401.

47. Anseth, K. S.; Wang, C. M.; Bowman, C. N., Reaction Behaviour and Kinetic Constants for Photopolymerizations of Multi (Meth) Acrylate Monomers. *Polymer* **1994,** *35*, 3243-3250.

48. Russell, G. T.; Napper, D. H.; Gilbert, R. G., Termination in Free-Radical Polymerizing Systems at High Conversion. *Macromolecules* **1988,** *21*, 2133-2140.

49. Bueche, F., *Physical Properties of Polymers*. Interscience Publishers: New York, **1962**.

50. Young, J. S.; Bowman, C. N., Effect of Polymerization Temperature and Cross-Linker Concentration on Reaction Diffusion Controlled Termination. *Macromolecules* **1999,** *32*, 6073-6081.

51. Wen, M.; McCormick, A. V., A Kinetic Model for Radical Trapping in Photopolymerization of Multifunctional Monomers. *Macromolecules* **2000,** *33*, 9247-9254.

UV intensity (mW/cm^2)	D_n (%)	$R_B P_n$ (%)	$P_n^{\bullet}$ (%)
0,01	28	39	33
0,1	27	56	17
1	35	56	9
3	59	36	5

Table 1: Relative fractions of terminated species and macroradicals at the end of polymerization process.

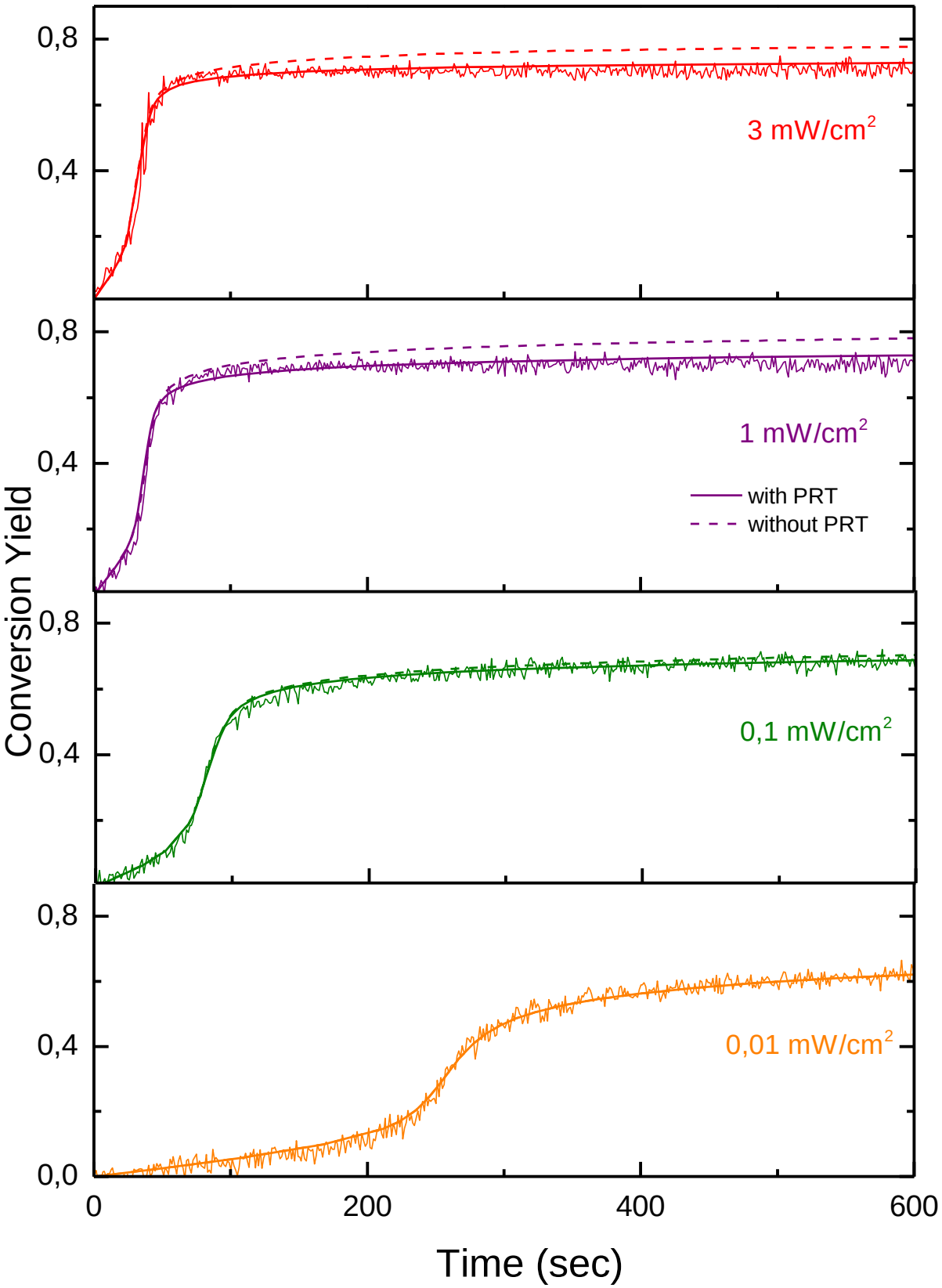

Figure 1: : Temporal variation of double bond conversion yield at several UV intensities. Simulations results with (solid line) and without (dashed line) PRT process are also indicated.

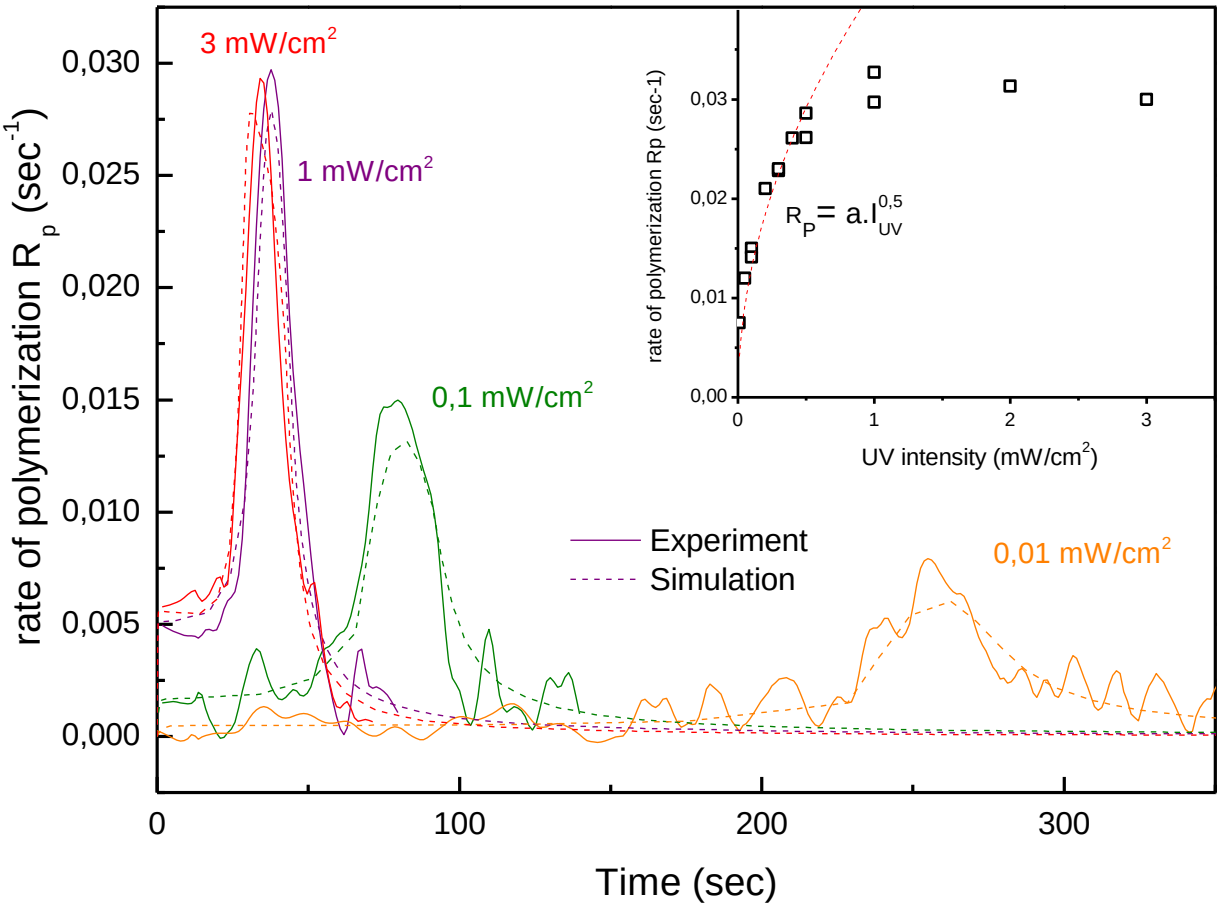

Figure 2 : Comparison of experimental and simulated rates of polymerization vs time. Insert shows maximum rate of polymerization vs UV intensity. The dashed line traces 1/2 power variation of intensity.

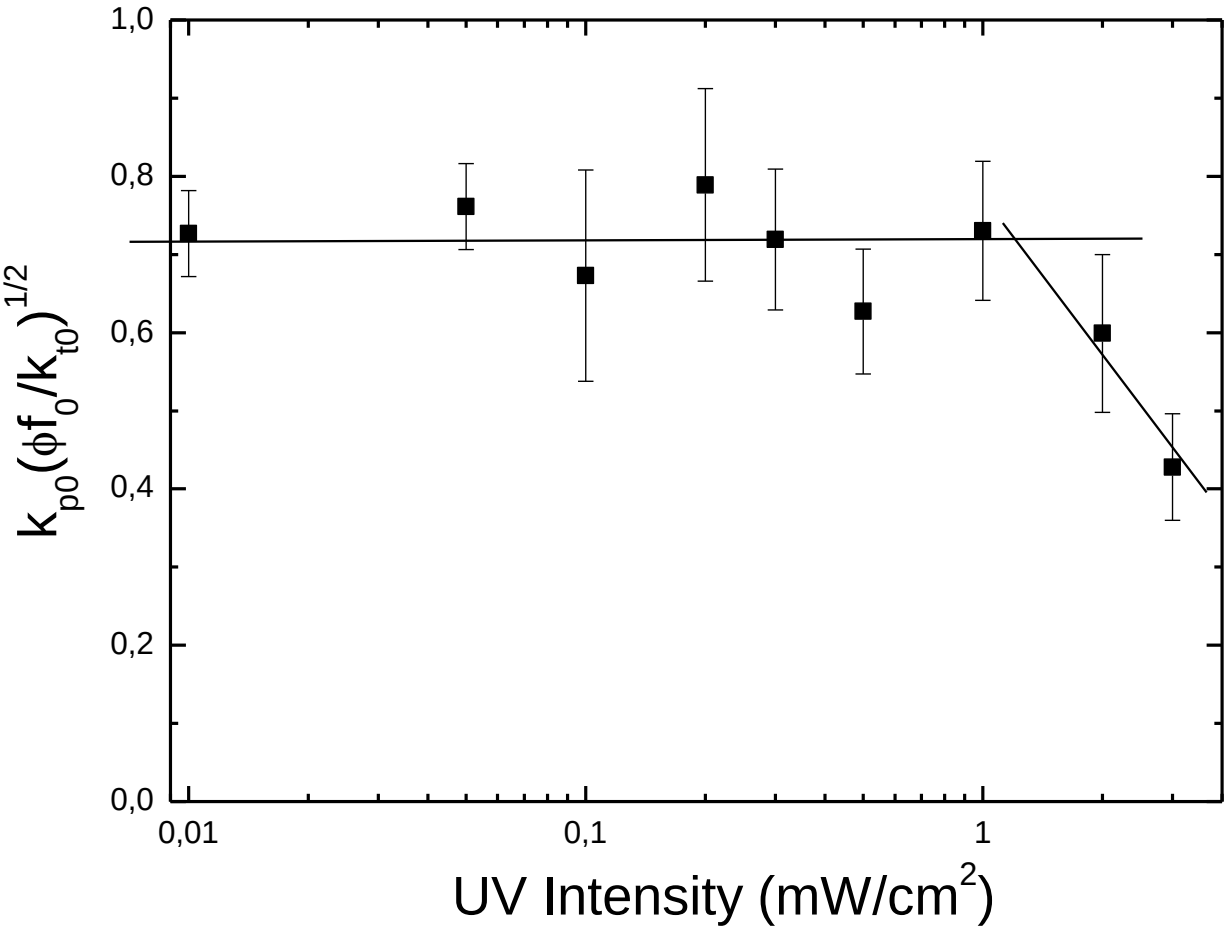

Figure 3: Factor $k_{p0}\sqrt{f_0\phi/k_{t0}}$ (calculated in the process beginning using experimental data) vs UV light intensity.

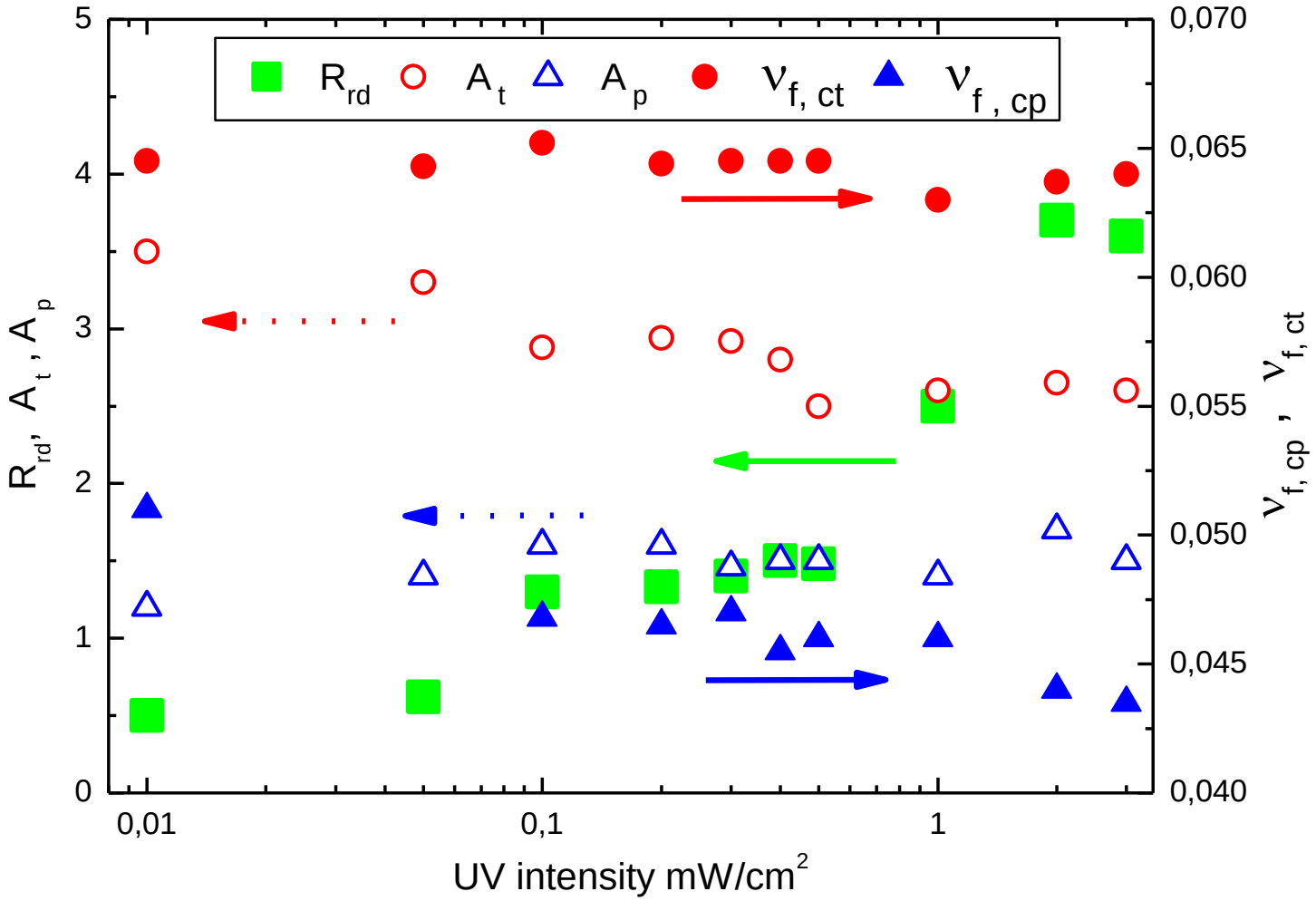

Figure 4 : Values of diffusion controlled parameters vs UV light intensity.

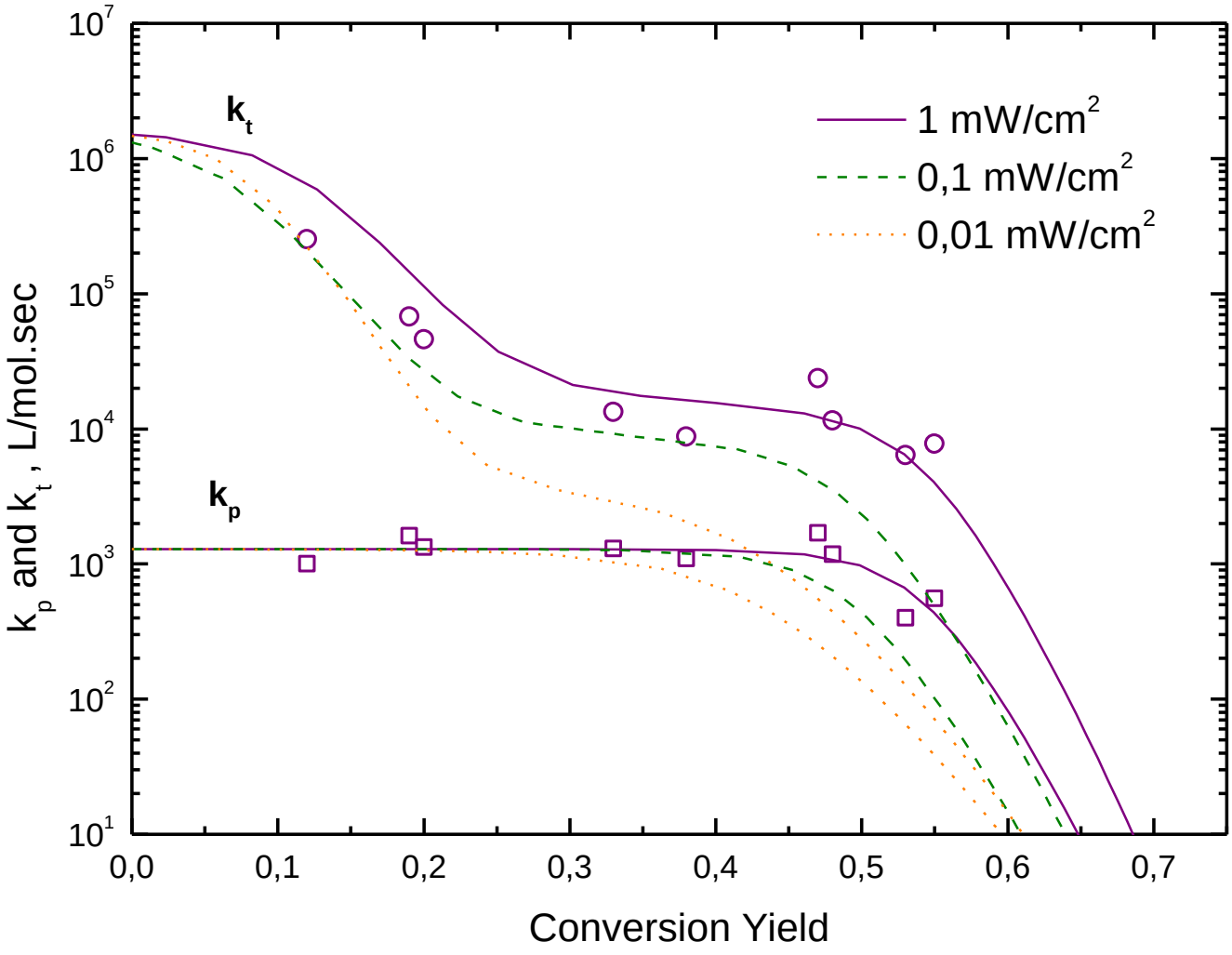

Figure 5: Variation of propagation kp and bimolecular termination kt rate constants estimated from eqs (13) and (14) vs conversion yield at different UV intensities. The symbols (□) and (O) show the experimentally measured rate constants (I_{UV} = 1 mW/cm^2) (see the text for details).

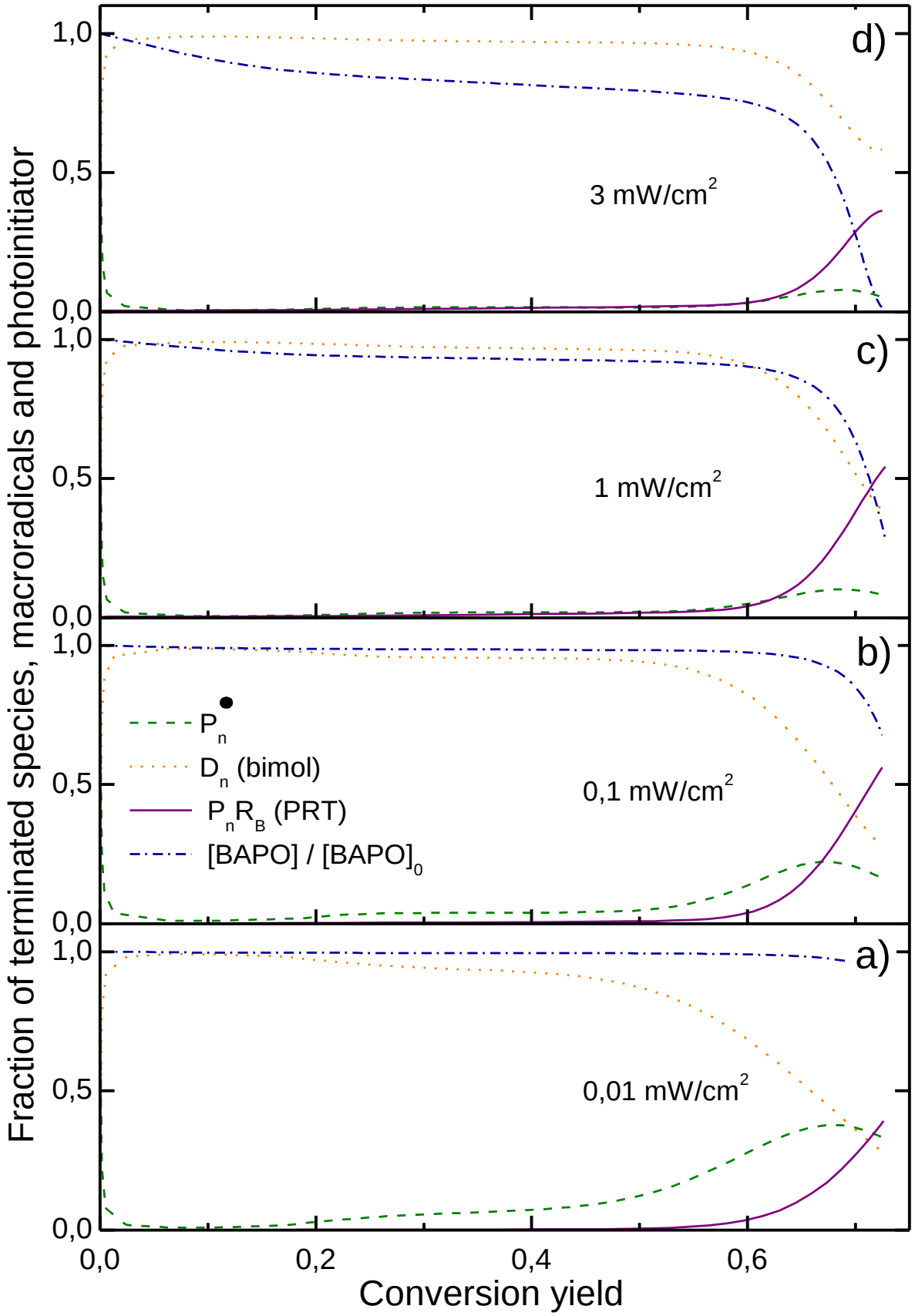

Figure 6. Fraction of terminated species and macroradicals as a function of conversion yield. Relative concentration of photoinitiator is also shown.

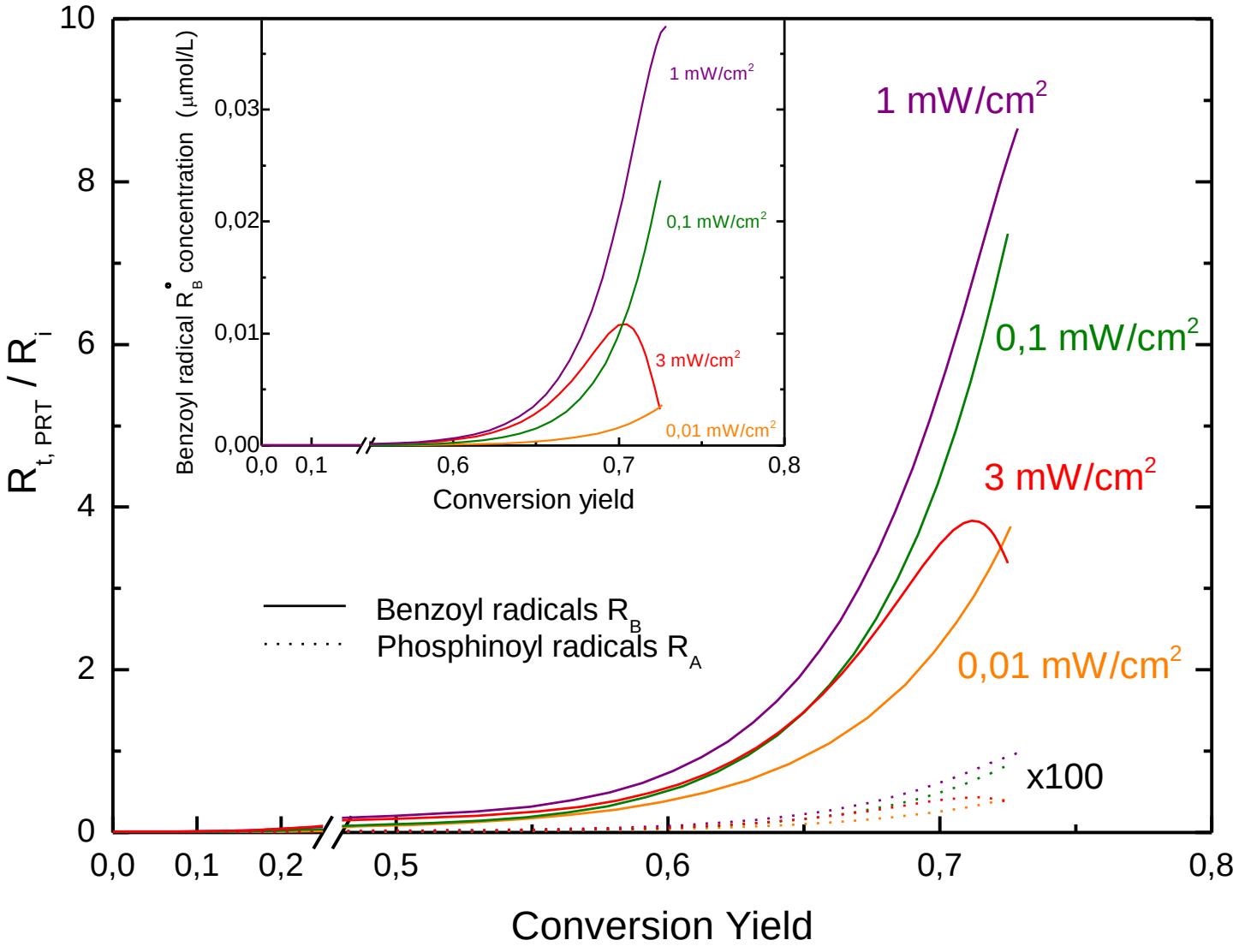

Figure 7: Evolution of ratio R_{PRT} / R_i for benzoyl (solid line) and phosphinoyl (dotted line) radicals as a function of double bond conversion at different UV intensities. Insert shows variation of benzoyl radical concentration as function of conversion yield.

TOC Graphic

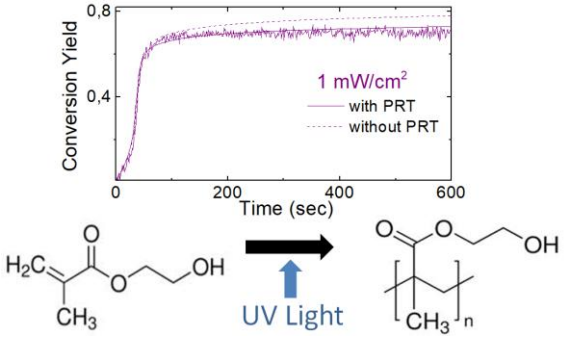
Conversion Yield
0,8
0,4
0
200
400
600
Time (sec)
1 mW/cm2
with PRT
without PRT
H2C
O
O
OH
CH3
UV Light
O
O
OH
CH3
n